Aquat Geochem (2007) 13:309–338
DOI 10.1007/s10498-007-9022-z

ORIGINAL PAPER

Dissolution Kinetics of Dolomite in Water at Elevated Temperatures

Ronghua Zhang · Shumin Hu · Xuetong Zhang · Wenbin Yu

Received: 12 May 2006 / Accepted: 2 October 2007 / Published online: 1 November 2007

Abstract Kinetic experiments of dolomite dissolution in water over a temperature range from 25 to 250°C were performed using a flow through packed bed reactor. Authors chose three different size fractions of dolomite samples: 18–35 mesh, 35–60 mesh, and 60–80 mesh. The dissolution rates of the three particle size samples of dolomite were measured. The dissolution rate values are changed with the variation of grain size of the sample. For the sample through 20–40 mesh, both the release rate of Ca and the release rate of Mg increase with increasing temperature until 200°C, then decrease with continued increasing temperature. Its maximum dissolution rate occurs at 200°C. The maximum dissolution rates for the sample through 40–60 mesh and 60–80 mesh happen at 100°C. Experimental results indicate that the dissolution of dolomite is incongruent in most cases. Dissolution of fresh dolomite was non-stoichiometric, the Ca/Mg ratio released to solution was greater than in the bulk solid, and the ratio increases with rising temperatures from 25 to 250°C. Observations on dolomite dissolution in water are presented as three parallel reactions, and each reaction occurs in consecutive steps as

$$\mathrm{CaMg(CO_3)_2(s) = MgCO_3(s) + Ca^{2+} + CO_3^{2-}}$$

$$\mathrm{MgCO_3(s) = Mg^{2+} + {CO_3}^{2-}}$$

where the second part is a slow reaction, and also the reaction could occur as follows:

$$\mathrm{CaMg(CO_3)_2(s) + Mg^{2+} = Ca^{2+} + 2MgCO_3(s)}$$

The following rate equation was used to describe dolomite dissolution kinetics

$$\mathrm{Rate} = \Sigma r_{ij} = \Sigma k_{ij}(a_i)^n$$

where Σr_{ij} refers to one of each reaction among the above reactions; k_{ij} is the rate constant for ith species in the jth reaction, a_i stands for activity of ith aqueous species, n is the stoichimetric coefficience of ith species in the jth reaction, and define $n = n_{ij}$.

R. Zhang (✉) · S. Hu · X. Zhang · W. Yu
Open Research Laboratory of Geochemical Kinetics, Chinese Academy of Geological Sciences, Institute of Mineral Resources, Baiwanzhuang Road 26, Beijing 100037, China
e-mail: zrhhsm@pku.edu.cn

The experiments prove that dissolved Ca is a strong inhibitor for dolomite dissolution (release of Ca) in most cases. Dissolved Mg was found to be an inhibitor for dolomite dissolution at low temperatures. But dissolution rates of dolomite increase with increasing the concentration of dissolved Mg in the temperature range of 200–250°C for 20–40 mesh sample, and in the temperature range of 100–250°C for 40–80 mesh sample, whereas the Mg^{2+} ion adsorption on dolomite surface becomes progressively the step controlling reaction. The following rate equation is suitable to dolomite dissolutions at high temperatures from 200 to 250°C.

$$-r_{Ca^{2+}} = k(m_{Ca^{2+}})^n + k_{ad}(K_{Mg^{2+}} m_{Mg^{2+}})/(1 + K_{Mg^{2+}} m_{Mg^{2+}})$$

where $-r_{Ca^{2+}}$ refers to dissolution rate (release of Ca), $m_{Ca^{2+}}$ and $m_{Mg^{2+}}$ are molar concentrations of dissolved Ca and Mg, k_{ad} stands for adsorption reaction rate constant, K_{Mg} refers to adsorption equilibrium constant.

At 200°C for 40–60 mesh sample, the release rate of Ca can be described as:

$$-r(\mathrm{mol\,m^{-2}\,s^{-1}}) = 0.55 \times 10^{-4}(m_{Ca})^{-0.36} + 0.135 \times 10^{-4}(m_{Mg})/(1 + 0.14\, m_{Mg})$$

Keywords Dolomite · High temperature · Dissolution kinetics · Release rate · Adsorption reaction

1 Introduction

Dolomite dissolution kinetics at elevated temperatures has been rarely studied. For a complete understanding of the geochemistry of dolomite aquifers, evolution of karst landforms, carbonate diagenesis, and dolomitization in epithermal deposits, an experimental study of dolomite dissolution kinetics over a temperature range of 25–250°C is required.

Previous studies of dolomite dissolution were conducted in solutions of HCl at temperatures ≤100°C (Lund et al. 1973; Busenberg and Plummer 1982). Their observations were described an empirical relation

$$\mathrm{Rate} = k(a_{H^+})^n \tag{1}$$

The reaction of adsorbed H^+ with solid is the slow step. Rate refers to overall dissolution rate. The n is exponent number, and k stands for rate constant. Generally, dolomite dissolution can be destributed by three parallel reactions occurring at the solid/water interface (Plummer Wigler and Parkhurst 1978; Chou et al. 1989; Wollast 1990)

$$CaMg(CO_3)_2 + 2H^+ \xrightarrow{k_1} Mg^{2+} + Ca^{2+} + 2HCO_3^- \tag{2}$$

$$CaMg(CO_3)_2 + 2H_2CO_3 \xrightarrow{k_2} Mg^{2+} + Ca^{2+} + 4HCO_3^- \tag{3}$$

$$CaMg(CO_3)_2 \underset{k_{3-}}{\overset{k_3}{\leftrightarrow}} Mg^{2+} + Ca^{2+} + 2CO_3^{2-} \tag{4}$$

Assuming dolomite precipitation is expressed by the third reaction, then

$$\mathrm{Rate} = k_1 a_{H^+}^n + k_2 a_{H_2CO_3}^p + k_3 - k_{-3} a_{Mg^{2+}} a_{Ca^{2+}} a_{CO_3^{2-}}^2 \tag{5}$$

The exponent n varies from 0.5 (Busenberg and Plummer 1982) to 0.75 (Chou et al. 1989). And whereas p is equal 0.5–1 (Chou et al. 1989; Busenberg and Plummer 1982). The first term for Eq. 2 corresponds to dolomite surface protonation, the second term to its carbonatation, the third term to surface hydration, and the fourth term accounts for the precipitation reaction.

Busenberg and Plummer (1982) reported that dissolution of fresh dolomite was non-stoichiometric, the Ca/Mg ratio released to solution was greater than in the bulk solid. This effect of an apparently more rapid reaction with the $CaCO_3$ component of dolomite was very short-lived. A reaction mechanism consistent with all observations was presented as three parallel reactions of dolomite reacting with H^+, H_2CO_3 and H_2O, respectively, to form dissolved species. But each reaction occurs in consecutive steps as:

$$CaMg(CO_3)_2(s) + H^+ = MgCO_3(s) + Ca^{2+} + HCO_3^- \quad (6)$$

$$MgCO_3(s) + H^+ = Mg^{2+} + HCO_3^- \quad (7)$$

where the second part is a slow reaction, and also the reaction could occur as follows:

$$CaMg(CO_3)_2(s) + Mg^{2+} = Ca^{2+} + 2MgCO_3(s) \quad (8)$$

Hermen and White (1985) carried out the experiments of the dissolution kinetics of three stoichiometric dolomite specimens (hydrothermal single crystal, microcrystalline sedimentary rock, coarse-grained marble) in aqueous carbonate solutions using a rotating dolomite disk. The dissolution rate values are changed with the variation of grain size of the sample and the spinning speed. But the spinning speed became a less important factor as the saturation state of the solutions increased as the temperature decreased.

In order to distinguish and to measure transport rates and chemical reaction rates for carbonate dissolutions, scientists have used the different flow reactor or rotating-disc apparatus, which allow us a precise definition of the hydrodynamics of the experimental system (Sjöberg and Rickard 1984; Casey 1987; Chou et al. 1989; Morphy et al. 1989; Zhang et al. 1992, 1993, 1998). And it also reveals that the dissolution rates depend critically on the ratio V/A of the volume V of the so1ution and the surface area of the reacting minera1 A (Buhmann and Dreybrodt 1985a, b; Zhang et al. 1990a, b).

Recently, Pokrovsky and Schott (2001) measured dolomite dissolution rates at 25°C, and found in the alkaline pH region, dolomite dissolution is not independent on pH, and carbonate and bicarbonate ions significantly inhibit dissolution rates at far from equilibrium conditions. It was found that dissolved Ca is a strong inhibitor of dolomite dissolution at $pH > 7$, whereas dissolved Mg has no effect on the dissolution rate. The surface complexation model (Pokrovsky et al. 1999) was used to correlate dissolution kinetics with surface speciation. At the conditions ($5 < pH \leq 12$) dolomite dissolution is controlled by the hydration of Mg surface sites. This is in agreement with the suggestion by Busenberg and Plummer (1982) that dolomite dissolution is controlled by the protonation and hydrolysis of its $MgCO_3$ sites.

Authors carried out experiments of dolomite dissolution in water over the temperature ranges 25–250°C using a flow through apparatus, Packed Bed Reactor, in an open system. The experiments provide new data that dolomite dissolution rates vary with temperature and with the variation of grain size of the sample. In these experiments of dolomite dissolution in neutral solution, authors would not enable to investigate how dolomite dissolution rates vary with pH and fugacity of CO_2. Experiments indicate both dissolved Ca in solution and Mg adsorption on dolomite surface will inhibit the

dissolving of dolomite, but the mechanism of dissolution of dolomite at low temperatures differs from that at high temperatures.

2 Experimental Procedures

2.1 Sample Preparation

Dolomite samples were obtained from Geological Museum, Beijing. They are white color and quite large crystals (2–5 mm). The dolomite particles were crashed into a ceramic shatter box and sieved to 20–40, 40–60, and 60–80 mesh, then the pure crystals were hand-picked under microscope observation. Dolomite composition is listed in Table 1. And also, the mineral particles were cleaned ultrasonically using acetone to remove fine particles, rinsed with distilled water and dried at 70–80°C. Then surface areas of representative samples were determined by a single point (Kr–He) BET method. The surface area for dolomite particles through 20–40 mesh is 0.5 m^2/g; the surface area through 40–60 mesh is 0.8 m^2/g; the surface area through 60–80 mesh is 0.78 m^2/g.

2.2 Apparatus

The equipment used during the laboratory experiments duplicated that used in previous studies (Zhang et al. 1990a, b, 1992; Zhang and Hu 1996) and included a pressure vessel, liquid pump, back pressure regulator, temperature controller, heat source (furnace), pressure gauge, electric conductivity detector, and computer (Fig. 1).

Mineral particles were introduced to the pressure vessel, which was mounted vertically. De-ionized and degassed water was derived into the vessel from the bottom to the top at different flow rates (0.5–3 ml/min). Time is measured in the experiments with unit min. Output solutions were sampled and the composition of these solutions was analyzed. Note: the continuous flow reactor incorporates a continuous input of aqueous solutions through a packed mineral bed and a resulting continuous fluid output. Within the packed bed reactor, a transient material balance in a column at length Z gives:

$$D_L \frac{\partial^2 C}{\partial Z^2} - U\frac{\partial C}{\partial Z} + r = \frac{\partial C}{\partial t} \tag{9}$$

where D_L refers to the axial dispersion coefficient (diffusion process involved), U is the flow rate, C is the concentration, r is the reaction rate ((mol/min) or (mol/min/m^2) or (mol/s/m^2)). The output solutions pass through an electric conductivity detector, and a computer monitor displays the continuous variation of the electric conductivity of the output solutions in the reaction system, which indicates whether the system is at a steady state or not. As $\partial C/\partial t = 0$, the system is at a steady state, i.e., the electric conductivity of the outlet fluids is constant. At this time, liquid products of the system were sampled (Zhang et al. 1989, 1990a, b, 1992, 1998). This model reflects mass transfer in axial

Table 1 Chemical composition of dolomite

SiO_2	Al_2O_3	Fe_2O_3	FeO	MgO	CaO	Na_2O	K_2O	H_2O	H_2O	TiO_2	P_2O_5	MnO	CO_2	Ca/Mg	Σ
1.91	0.652	0.3	3.54	18.25	29.69	0.14	0.018	0.089	0	0.012	0.046	0.46	43.98	1.17	99.27

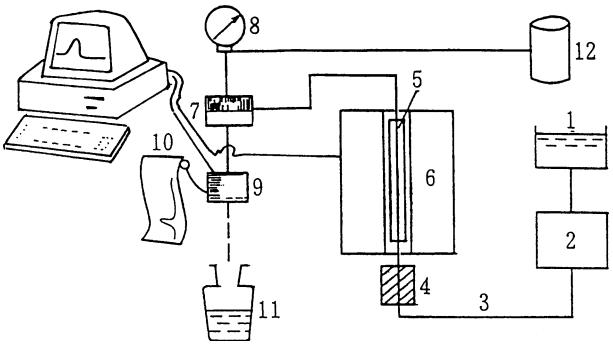

Fig. 1 Schematic illustration of the experimental approach used in the present study to perform open system experiments (see text). (1) liquid reservoir; (2) pump; (3) titanium tubing; (4) preheating; (5) titanium vessel; (6) furnace; (7) back pressure regulator; (8) pressure gauge; (9) electronic conductivity detector and recorder; (10) computer control; (11) sample outlet; (12) gas cylinder

direction in terms of an effective longitudinal diffusivity superimposed on the plug flow reactor velocity. This equation can also describe the natural process coupling of advection or flowing, diffusion or dispersion, and rock-fluid interaction in a porous media of rocks. The previous study had measured the average residence time at each flow rate in the flow through packed bed reactor after having put mineral particles in the vessel (Zhang et al. 1992).

This kind of experimental system has been used to perform kinetic experiments previously, or it is called column experiment (Cama et al. 1999; Hellmann 1995; Hellmann et al. 1989; Mogollon et al. 1996, 2000; Weissbart and Rimstidt 2000; Zhang and Hu 1996; Zhang et al. 1990a, b, 2000, 2002).

2.3 Sampling and Analysis

The experiments were operated under a steady state condition in the temperature range from 25 to 250°C and at constant pressure of 12.07 MPa. We maintained the temperature and pressure constant, and changed the flow rate from 0.08 to 3.5 ml/min, in an isothermal process. Then we took solution samples as often as every hour after changing a flow rate or changing a temperature in order to obtain aqueous solution product at steady state dissolution process in the system at constant temperature, constant pressure and constant flow rate. The calcium and magnesium concentrations of the output solutions were measured using ICP-MS (Table 2).

3 Experimental Results

3.1 Theoretical Consideration and Calculation Data

In this work, we maintained to input degassed and de-ionized water to the pressure vessel, and did not change the pH of input aqueous solution, therefore, (a_{H^+}) would be approximately constant. The initial pressure of CO_2 in water is zero, because we pump in de-ionized and degassed water. The partial pressure of CO_2 inside of pressure vessel is

Table 2 Kinetic experimental results of dolomite dissolution in water

Number	T (°C)	Aver. time (min)	$m_{Ca^{2+}}$	$m_{Mg^{2+}}$	Rate (Ca) (mol/m^2/s) × 10^{-5}	Rate (Mg) (mol/m^2/s) × 10^{-5}
20–40 mesh						
1	25	29.61	2.225	0.6875	0.0005367	0.0001658
2	25	35.04	2.04	0.4792	0.0004159	9.768E-05
3	25	3.28	1.3275	0.2083	0.0028909	0.0004536
4	25	3.31	1.3275	0.2083	0.0028647	0.0004495
5	25	3.25	1.3275	0.2083	0.0029176	0.0004578
6	25	1.95	1.02	0.225	0.0037363	0.0008242
7	25	1.95	1.02	0.1958	0.0037363	0.0007172
8	25	1.9	1.02	0.1917	0.0038346	0.0007207
9	25	1.39	0.8675	0.1917	0.0044579	0.0009851
10	25	1.38	0.8675	0.1917	0.0044902	0.0009922
11	25	1.38	0.8675	0.1875	0.0044902	0.0009705
12	25	1.38	0.715	0.1708	0.0037008	0.0008841
13	25	1.1	0.715	0.1708	0.0046429	0.0011091
14	25	1.1	0.715	0.1667	0.0046429	0.0010825
15	25	1.01	0.61	0.1625	0.004314	0.0011492
16	25	1.02	0.56	0.1667	0.0039216	0.0011674
17	25	1.02	0.61	0.1625	0.0042717	0.001138
18	55	19.69	2.3475	0.5417	0.0008516	0.0001965
19	46	20.66	1.8375	0.5833	0.0006353	0.0002017
20	90	20.18	2.705	0.8667	0.0009575	0.0003068
21	95	21.18	2.805	0.8667	0.000946	0.0002923
22	98	3.03	2.295	0.9417	0.0054102	0.0022199
23	98	3.69	2.295	0.9125	0.0044425	0.0017664
24	95	3.74	2.3475	0.9292	0.0044834	0.0017746
25	95	2.06	1.917	0.7917	0.006647	0.0027451
26	95	2.04	1.8875	0.7583	0.0066089	0.0026551
27	90	2.04	1.8375	0.7458	0.0064338	0.0026113
28	96	1.42	1.53	0.575	0.0076962	0.0028924
29	96	1.44	1.3773	0.5458	0.0068318	0.0027073
30	95	1.43	1.3275	0.5375	0.0066309	0.0026848
31	102	1.13	1.225	0.4625	0.0077434	0.0029235
32	102	1.13	1.1725	0.4083	0.0074115	0.0025809
33	98	1.13	1.12	0.4125	0.0070796	0.0026075
34	100	1.02	1.07	0.3792	0.007493	0.0026555
35	97	1.07	1.07	0.3833	0.0071429	0.0025587
36	95	1.02	0.97	0.3708	0.0067927	0.0025966
37	46	20.12	1.99	0.65	0.0007065	0.0002308
38	50	3.55	1.1725	0.4125	0.0023592	0.00083
39	46	3.63	1.12	0.4	0.0022039	0.0007871
40	46	3.55	1.1725	0.395	0.0023592	0.0007948
41	50	2.03	0.97	0.333	0.0034131	0.0011717

Table 2 continued

Number	T (°C)	Aver. time (min)	$m_{Ca^{2+}}$	$m_{Mg^{2+}}$	Rate (Ca) (mol/m^2/s) $\times 10^{-5}$	Rate (Mg) (mol/m^2/s) $\times 10^{-5}$
42	52	2.02	1.07	0.3917	0.0037836	0.0013851
43	50	2.03	1.02	0.35	0.003589	0.0012315
44	48	1.43	0.765	0.3	0.0038212	0.0014985
45	47	1.44	0.765	0.3125	0.0037946	0.0015501
46	48	1.43	0.765	0.2958	0.0038212	0.0014775
47	50	1.13	0.6625	0.2667	0.0041877	0.0016858
48	50	1.13	0.6625	0.2625	0.0041877	0.0016593
49	48	1.12	0.6625	0.2625	0.0042251	0.0016741
50	50	1.02	0.61	0.2458	0.0042717	0.0017213
51	52	1.02	0.61	0.2417	0.0042717	0.0016926
52	52	1.01	0.56	0.2417	0.0039604	0.0017093
53	148	22.88	3.265	0.7708	0.0010193	0.0002406
54	155	22.27	3.265	0.8042	0.0010472	0.0002579
55	150	3.53	2.505	0.8292	0.0050688	0.0016779
56	152	3.55	2.5	0.8042	0.0050302	0.0016181
57	150	3.57	2.4875	0.7017	0.004977	0.001404
58	152	2.01	2.195	0.7292	0.0078003	0.0025913
59	150	2.03	2.1425	0.7292	0.0075387	0.0025658
60	148	2.03	2.1425	0.7292	0.0075387	0.0025658
61	150	1.32	1.6825	0.6125	0.0091044	0.0033144
62	150	1.43	1.6825	1.0166667	0.0084041	0.0050783
63	150	1.43	1.785	0.6083333	0.0089161	0.0030386
64	150	1.13	1.48	0.5041667	0.0093552	0.0031869
65	150	1.13	1.48	0.5041667	0.0093552	0.0031869
66	150	1.12	1.4275	0.525	0.009104	0.0033482
67	150	1.02	1.225	0.4541667	0.0085784	0.0031804
68	150	1.02	1.275	0.4541667	0.0089286	0.0031804
69	150	1.02	1.3275	0.4416667	0.0092962	0.0030929
70	200	29.13	3.52	0.3916667	0.0008631	9.604E-05
71	196	34.21	3.4175	0.35	0.0007136	7.308E-05
72	200	3.659	2.5	0.2041667	0.0048803	0.0003986
73	200	3.68	2.3975	0.0875	0.0046535	0.0001698
74	200	3.72	2.45	0.0625	0.0047043	0.00012
75	200	2.09	2.5	0.3291667	0.0085441	0.001125
76	200	2.1	2.2725	0.3458333	0.0077296	0.0011763
77	200	2.1	2.2725	0.4083333	0.0077296	0.0013889
79	195	1.42	2.3075	0.6958333	0.0116071	0.0035002
80	194	1.42	2.3075	0.6833333	0.0116071	0.0034373
81	194	1.42	2.215	0.6833333	0.0111419	0.0034373
82	195	1.12	2.035	0.5916667	0.0129783	0.0037734
83	200	1.12	2.035	0.6	0.0129783	0.0038265
84	196	1.12	1.9425	0.5916667	0.0123884	0.0037734

Table 2 continued

Number	T (°C)	Aver. time (min)	$m_{Ca^{2+}}$	$m_{Mg^{2+}}$	Rate (Ca) (mol/m^2/s) × 10^{-5}	Rate (Mg) (mol/m^2/s) × 10^{-5}
85	200	1.03	1.9425	0.6166667	0.0134709	0.0042765
86	198	1.02	1.9425	0.6166667	0.0136029	0.0043184
87	198	1.02	1.8975	0.5916667	0.0132878	0.0041433
88	250	54.19	2.6275	0.2916667	0.0003463	3.844E-05
89	247	8.99	2.17	0.0916667	0.0017241	7.283E-05
90	252	8.75	2.08	0.1083333	0.001698	8.844E-05
91	248	8.16	2.035	0.1333333	0.0017813	0.0001167
92	246	2.66	1.7625	0.0291667	0.0047328	7.832E-05
93	250	2.62	1.8075	0.0375	0.0049278	0.0001022
94	250	2.63	1.625	0.0208333	0.0044134	5.658E-05
95	247	1.68	2.035	0.1458333	0.0086522	0.00062
96	250	1.68	2.01	0.1291667	0.0085459	0.0005492
97	250	1.68	2.1025	0.0958333	0.0089392	0.0004075
98	250	1.67	1.8975	0.1	0.0081159	0.0004277
99	250	1.25	1.8525	0.1166667	0.0105857	0.0006667
100	248	1.25	1.8525	0.1291667	0.0105857	0.0007381
101	250	1.11	1.9425	0.2	0.0125	0.001287
102	248	1.11	1.9875	0.2583333	0.0127896	0.0016624
103	244	1.1	1.9875	0.3083333	0.0129058	0.0020022
104	25	12.6	1.215	0.4791667	0.0006888	0.0002716
105	25	13.81	1.215	0.4708333	0.0006284	0.0002435
106	25	3.25	1.035	0.3166667	0.0022747	0.000696
107	25	3.24	1.08	0.3041667	0.002381	0.0006706
108	25	3.24	1.035	0.3083333	0.0022817	0.0006797
109	25	1.93	0.9425	0.2458333	0.0034882	0.0009098
110	25	1.92	0.9425	0.2416667	0.0035063	0.0008991
111	25	1.75	0.9425	0.2458333	0.0038469	0.0010034
112	25	1.4	0.8525	0.2125	0.0043495	0.0010842
113	25	1.41	0.8525	0.2041667	0.0043186	0.0010343
114	25	1.4	0.8075	0.2083333	0.0041199	0.0010629
115	25	1.11	0.7625	0.1833333	0.0049067	0.0011798
116	25	1.11	0.7625	0.1875	0.0049067	0.0012066
117	25	1.11	0.7625	0.1875	0.0049067	0.0012066
118	25	1.01	0.67	0.1708333	0.0047383	0.0012082
119	25	1.01	0.715	0.175	0.0050566	0.0012376
120	25	1.01	0.625	0.1708333	0.0044201	0.0724894
40–60 mesh						
145	25	9.2	12.5	2.125	0.009643	0.001071
147	25	8.66	11.25	1.833	0.009286	0.000893
148	25	3.19	10	1.458	0.022321	0.001964
149	25	3.2	10	1.375	0.022321	0.001786
150	25	3.21	10	1.292	0.022321	0.001786

Table 2 continued

Number	T (°C)	Aver. time (min)	$m_{Ca^{2+}}$	$m_{Mg^{2+}}$	Rate (Ca) (mol/m^2/s) $\times 10^{-5}$	Rate (Mg) (mol/m^2/s) $\times 10^{-5}$
151	25	1.91	9.375	1.167	0.035	0.002679
152	25	1.91	9.375	1.292	0.035	0.002857
153	25	1.91	8.75	1.167	0.032679	0.002679
154	25	1.39	8.125	1.083	0.041786	0.003393
155	25	1.39	7.5	1.042	0.038571	0.003214
156	25	1.39	7.5	1	0.038571	0.003036
158	25	1.11	6.25	0.958	0.040179	0.00375
159	25	1.11	6.25	0.917	0.040179	0.00375
160	25	1.11	6.25	0.875	0.040179	0.003571
161	25	1.01	6.25	0.875	0.044286	0.003929
162	25	1.01	5.625	0.875	0.039821	0.003929
163	25	1.01	5.625	0.875	0.039821	0.003929
165	50	7.1	18.125	5.542	0.018214	0.003018
166	50	7.12	20.625	6.875	0.020714	0.004107
167	50	3.25	20.625	5.292	0.045357	0.006964
168	50	3.25	16.25	5.25	0.035714	0.006964
169	50	3.26	16.25	5.208	0.035714	0.006786
170	50	1.94	13.125	3.583	0.048393	0.007857
171	50	1.94	13.125	3.667	0.048393	0.008036
172	50	1.94	13.125	3.583	0.048393	0.007857
173	50	1.4	10.625	2.75	0.054286	0.008393
174	50	1.4	10.625	2.583	0.054286	0.007857
175	50	1.4	10.625	2.583	0.054286	0.007857
176	50	1.11	9.375	2.375	0.060357	0.009107
177	50	1.11	9.375	2.5	0.060357	0.009643
178	50	1.11	9.375	2.5	0.060357	0.009643
179	50	1.01	8.75	2.708	0.061964	0.011429
180	50	1.01	9.525	2.5	0.067321	0.010536
181	50	1.01	10	2.917	0.070714	0.012321
182	100	7.05	26.25	9.042	0.026607	0.005536
183	100	7.11	25.625	9.417	0.025714	0.005714
184	100	3.22	25.625	9.458	0.056786	0.0125
185	100	3.22	25.625	9.5	0.056786	0.012679
186	100	3.22	25	9.25	0.055536	0.012321
187	100	1.92	23.75	9.625	0.088393	0.021429
188	100	1.91	23.125	9.667	0.086429	0.021607
189	100	1.91	23.75	9.25	0.08875	0.020714
190	100	1.37	21.25	8.792	0.11	0.027321
191	100	1.38	21.875	8.958	0.113214	0.027857
192	100	1.38	21.25	8.792	0.11	0.027321
193	100	1.1	20.625	8.958	0.133929	0.034821
194	100	1.1	20	8.958	0.129821	0.034821

Table 2 continued

Number	T (°C)	Aver. time (min)	$m_{Ca^{2+}}$	$m_{Mg^{2+}}$	Rate (Ca) (mol/m^2/s) $\times 10^{-5}$	Rate (Mg) (mol/m^2/s) $\times 10^{-5}$
195	100	1.1	20.625	9.042	0.133929	0.035179
196	100	1	20	8.625	0.142857	0.036964
197	100	1	18.75	8.833	0.133929	0.037857
198	100	1	18.75	8.75	0.133929	0.0375
199	150	7.07	25	4.958	0.025179	0.003036
200	150	7.03	23.125	3.792	0.023571	0.002321
201	150	3.22	22.5	5.833	0.049821	0.007679
202	150	3.23	22.5	6	0.049643	0.008036
203	150	3.25	21.875	6.417	0.048036	0.008393
204	150	1.93	22.5	7.875	0.083214	0.0175
205	150	1.93	21.875	8	0.080893	0.017679
206	150	1.93	21.25	8.083	0.078571	0.018036
207	150	1.39	20	8.792	0.102679	0.027143
208	150	1.39	20	8.875	0.102679	0.027321
209	150	1.39	19.375	9.167	0.099464	0.028214
210	150	1.1	16.875	8.958	0.109643	0.034821
211	150	1.1	17.5	8.958	0.113571	0.034821
212	150	1.1	16.875	8.917	0.109643	0.034821
213	150	1	15.625	8.875	0.111607	0.038036
214	150	1	15	8.875	0.107143	0.038036
215	150	1	15.625	9.125	0.111607	0.039107
216	200	7.02	27.5	0.667	0.028036	0.000357
217	200	7.07	26.875	0.542	0.027143	0.000357
218	200	3.42	22.5	0.542	0.046964	0.000714
219	200	3.39	21.875	0.583	0.046071	0.000714
220	200	3.4	24.625	0.667	0.043393	0.000893
221	200	2	20	0.917	0.071429	0.001964
222	200	2	20	0.958	0.071429	0.002143
223	200	2	19.375	1	0.069196	0.002321
224	200	1.44	17.5	1.875	0.086786	0.005536
225	200	1.43	17.5	2.208	0.0875	0.006607
226	200	1.43	17.5	2.333	0.0875	0.006964
227	200	1.13	17.5	3.167	0.110536	0.011964
228	200	1.13	16.875	3.667	0.106607	0.013929
229	200	1.13	16.875	4.333	0.106607	0.016429
230	200	1.02	16.875	8.375	0.118214	0.035179
231	200	1.02	16.2	8.542	0.113393	0.035893
232	200	1.02	16.25	8.958	0.11375	0.037679
233	250	7.65	27.5	0.417	0.025536	0.000179
234	250	7.77	26.25	0.125	0.024107	6.79E-05
235	250	5.39	22.5	Low	0.029821	0
236	250	5.45	21.875	Low	0.02875	0

Table 2 continued

Number	T (°C)	Aver. time (min)	$m_{Ca^{2+}}$	$m_{Mg^{2+}}$	Rate (Ca) (mol/m^2/s) $\times 10^{-5}$	Rate (Mg) (mol/m^2/s) $\times 10^{-5}$
237	250	5.35	21.25	Low	0.028393	0
238	250	2.45	15	Low	0.04375	0
239	250	2.43	14.375	0.075	0.042321	7.32E-05
240	250	2.41	15	0.075	0.036964	7.32E-05
241	250	1.6	12.5	0.125	0.055893	0.000357
242	250	1.59	12.5	0.083	0.056071	0.000179
243	250	1.6	11.25	0.083	0.050179	0.000179
244	250	1.2	10	0.125	0.059464	0.000446
245	250	1.2	10.625	0.167	0.063214	0.000536
246	250	1.19	10.625	0.25	0.06375	0.000893
247	250	1.07	10.625	0.167	0.070893	0.000714
248	250	1.07	10.625	0.208	0.070893	0.000893
249	250	1.07	11.25	0.25	0.075179	0.001
250	25	9.73	11.875	3	0.00875	0.00125
251	25	8.92	11.875	2.875	0.009464	0.001429
252	25	3.52	11.875	1.583	0.024107	0.001964
253	25	3.51	11.25	1.5	0.022857	0.001786
254	25	3.54	11.875	1.5	0.023929	0.001786
255	25	2.01	10.625	1.5	0.037679	0.003214
256	25	1.99	11.875	1.5	0.042679	0.003214
257	25	2.01	11.875	1.5	0.042143	0.003214
258	25	1.43	11.25	1	0.05625	0.003036
259	25	1.43	11.25	0.958	0.05625	0.002857
260	25	1.43	11.25	0.958	0.05625	0.002857
261	25	1.13	10.7	0.917	0.067679	0.003393
262	25	1.13	11.25	0.875	0.071071	0.003393
263	25	1.13	10.625	0.875	0.067143	0.003393
264	25	1.02	10.625	0.875	0.074464	0.00375
265	25	1.03	10.625	0.917	0.07375	0.00375
266	25	1.02	10.625	0.875	0.074464	0.00375
60–80 mesh						
268	25	7.17	14.175	4.292	0.014107	0.0025
269	25	7.92	14.5	4.083	0.013036	0.002143
270	25	3.25	13.275	2.125	0.029107	0.002857
271	25	3.23	13.275	2.042	0.029286	0.002679
272	25	3.25	12.95	2.042	0.028393	0.002679
273	25	1.93	11.725	1.475	0.043393	0.003929
274	25	1.93	12.025	1.708	0.044464	0.00375
275	25	1.92	11.725	1.667	0.043393	0.00375
276	25	1.39	11.4	1.458	0.058571	0.004464
277	25	1.39	11.4	1.458	0.058571	0.004464
278	25	1.39	11.725	1.458	0.060179	0.004464

Table 2 continued

Number	T (°C)	Aver. time (min)	$m_{Ca^{2+}}$	$m_{Mg^{2+}}$	Rate (Ca) (mol/m^2/s) $\times 10^{-5}$	Rate (Mg) (mol/m^2/s) $\times 10^{-5}$
279	25	1.1	11.1	1.333	0.072143	0.005179
280	25	1.11	11.4	1.292	0.073393	0.005
281	25	1.11	11.1	1.292	0.071429	0.005
282	25	1	9.55	1.25	0.068214	0.005357
283	25	1.01	9.875	1.292	0.069821	0.005536
284	25	1	9.875	1.292	0.070536	0.005536
286	50	7.23	16.35	7.875	0.016071	0.004643
287	50	7.17	16.025	7.958	0.015893	0.004821
288	50	3.24	16.35	7.958	0.036071	0.010536
289	50	3.23	16.65	7.958	0.036786	0.010536
290	50	3.24	17.875	7.958	0.039464	0.010536
291	50	1.92	17.275	6.792	0.064286	0.015179
292	50	1.93	17.875	6.542	0.066071	0.014464
293	50	1.91	16.65	6.542	0.062321	0.014643
294	50	1.38	15.1	5.792	0.078214	0.018036
295	50	1.47	14.8	6.333	0.071964	0.018393
296	50	1.53	12.65	6.292	0.059107	0.017679
297	50	1.11	12.65	5.333	0.081429	0.020536
298	50	1.1	12.65	5	0.081429	0.019464
299	50	1.11	12.325	4.833	0.079286	0.01875
300	50	1.01	11.725	3.667	0.082857	0.015536
301	50	1	11.4	3.583	0.081429	0.015357
302	50	1	11.725	3.5	0.08375	0.015
303	100	7.16	21.575	8.167	0.021607	0.004821
304	100	7.16	21.9	7.375	0.021786	0.004464
305	100	3.23	17.575	8.417	0.038929	0.01125
306	100	3.26	17.275	8.417	0.037857	0.011071
307	100	3.23	17.575	8.292	0.038929	0.011071
308	100	1.91	16.025	8.333	0.06	0.01875
309	100	2.06	15.725	8.75	0.054464	0.018214
310	100	1.92	15.725	8.75	0.059643	0.026964
311	100	1.39	15.725	8.458	0.080893	0.026071
312	100	1.39	15.725	8.583	0.080893	0.026429
313	100	1.369	15.725	8.583	0.080893	0.026429
314	100	1.1	14.8	8.375	0.096071	0.032679
315	100	1.1	14.8	8.583	0.096071	0.033393
316	100	1.1	14.8	8.417	0.096071	0.032857
317	100	0.97	15.1	8.583	0.11125	0.037857
318	100	1.01	14.5	8.75	0.1025	0.037143
319	100	1.01	14.8	8.583	0.104643	0.036429
320	150	7.16	22.825	5.375	0.022857	0.003214
321	150	7.15	23.45	4.208	0.023393	0.0025

Table 2 continued

Number	T (°C)	Aver. time (min)	$m_{Ca^{2+}}$	$m_{Mg^{2+}}$	Rate (Ca) (mol/m^2/s) $\times 10^{-5}$	Rate (Mg) (mol/m^2/s) $\times 10^{-5}$
322	150	3.26	20.65	3.333	0.045179	0.004464
323	150	3.24	21.275	3.458	0.046964	0.004643
324	150	3.26	20.35	3.417	0.044643	0.004464
325	150	1.93	16.95	5.792	0.062679	0.012857
326	150	1.93	16.35	6.083	0.060536	0.013571
327	150	1.93	16.95	6.333	0.062679	0.014107
328	150	1.39	15.725	7.167	0.080893	0.022143
329	150	1.39	16.025	7.417	0.082321	0.022857
330	150	1.38	16.025	7.417	0.118571	0.023036
331	150	1.11	15.425	8.25	0.099286	0.031786
332	150	1.1	15.1	8.375	0.098036	0.032679
333	150	1.1	15.725	8.417	0.102143	0.032857
334	150	1	15.425	8.5	0.110179	0.036429
335	150	1	16.025	8.5	0.114464	0.036429
336	150	1	16.95	8.417	0.121071	0.036071
337	200	7.11	26.825	1.708	0.026964	0.001071
338	200	7.11	27.45	1.042	0.0275	0.000714
339	200	3.23	22.25	0.625	0.049821	0.000893
340	200	3.24	21.275	0.625	0.046964	0.000893
341	200	3.27	20.05	0.708	0.04375	0.000893
342	200	1.92	18.2	0.917	0.067679	0.001964
343	200	1.92	17.275	0.917	0.064286	0.001964
344	200	1.92	16.95	0.917	0.063036	0.001964
345	200	1.39	15.725	0.958	0.080893	0.003036
346	200	1.38	16.35	1	0.084643	0.003036
347	200	1.39	16.025	1.125	0.082321	0.003393
348	200	1.1	15.725	2.125	0.102143	0.008214
349	200	1.1	15.425	2.208	0.100179	0.008571
350	200	1.1	15.725	2.292	0.102143	0.008929
351	200				0	0
352	200	1	15.725	2.792	0.112321	0.011964
353	200	1	15.425	2.792	0.110179	0.011964
354	250	7.01	17.875	0.25	0.018214	0.000153
355	250	6.44	16.025	0.125	0.017857	8.32E-05
356	250	3.24	13.575	0.08	0.03	0.00011
357	250	3.23	13.575	0.04	0.03	5.52E-05
358	250	3.24	13.875	0.08	0.030536	0.00011
359	250	1.95	11.4	0.125	0.041786	0.000268
360	250	1.93	11.4	0.167	0.042143	0.000357
361	250	1.93	11.725	0.125	0.043393	0.000286
362	250	1.39	10.175	0.125	0.052321	0.000357
363	250	1.39	9.85	0.125	0.050536	0.000357

Table 2 continued

Number	T (°C)	Aver. time (min)	$m_{Ca^{2+}}$	$m_{Mg^{2+}}$	Rate (Ca) (mol/m^2/s) × 10^{-5}	Rate (Mg) (mol/m^2/s) × 10^{-5}
364	250	1.4	10.175	0.125	0.051964	0.000357
365	250	1.11	11.725	0.25	0.075536	0.000893
366	250	1.1	12.025	0.25	0.078036	0.000893
367	250	1.11	12.325	0.25	0.079286	0.000893
368	250	1.01	11.4	0.25	0.080536	0.001071
369	250	1.01	11.4	0.208	0.080536	0.000893
370	250	1.01	11.725	0.25	0.082857	0.001071
371	25	8.76	14.5	2.042	0.011786	0.001
372	25	8.46	14.175	2.167	0.011964	0.001071
373	25	3.3	13.575	1.75	0.029286	0.002321
374	25	3.26	13.575	1.625	0.029821	0.002143
375	25	3.27	1..875	1.708	0.030357	0.002321
376	25	1.89	13.575	1.083	0.05125	0.0025
377	25	1.93	13.575	1.125	0.050179	0.0025
378	25	1.91	14.175	1.083	0.053036	0.0025
379	25	1.39	14.8	0.875	0.076071	0.002679
380	25	1.39	15.425	0.833	0.079286	0.0025
381	25	1.39	16.35	0.875	0.084107	0.002679
382	25	1.1	16.65	0.792	0.108036	0.003036
383	25	1.1	16.35	0.792	0.106071	0.003036
384	25	1.1	15.725	0.792	0.102143	0.003036
385	25	1	15.1	0.792	0.107857	0.003393
386	25	1.01	13.575	0.833	0.096071	0.003571
387	25	1.01	14.5	0.833	0.1025	0.003571

Note: Aver. time refers to average residence time (min); $m_{(Ca^{2+})}$ and $m_{(Mg^{2+})}$ stand for concentrations of Ca and Mg in output solutions; Rate (Ca) and Rate (Mg) refer to dissolution rates of dissolved Ca and Mg, i.e., release rate

determined by the dissolving species of dolomite, such as HCO_3^-. According to the concentrations of dissolving species of Ca and Mg measured for each sample, the partial pressures can be calculated from the reaction equilibrium $H_2O + CO_2 = H^+ + HCO_3^-$ (Zhang et al. 1990a, b).

The dominate aqueous species of the dissolved Ca and Mg and their species activities at run temperatures were calculated from total concentrations of dissolved elements in output solutions of our kinetic experiments using Shvarov software HCh (Shvarov 1989). The theoretical calculation provides the activity coefficients of aqueous species in output solutions of the experiments. Calculated results indicate that dominate species is HCO_3^- in most cases and also obtained partial pressure of CO^2, activity coefficients of $HCO_3^-Ca^{2+}$ and Mg^{2+} in the experiment conditions at temperature range from 25°C to 250°C. The partial pressure of CO_2 is extremely low, due to small concentrations of dissolved Ca and Mg, e.g., 0.5–3.5 × 10^{-4} mol.

In this study, we predicted that dolomite surface protonation and carbonatation might be not important, and hydrolysis of its $MgCO_3$ sites would control dolomite dissolution.

Experimental results indicate that the dissolution of fresh dolomite was non-stoichiometric, the Ca/Mg ratio released to solution was greater than in the bulk solid (Sect. 3.2). Observations on dolomite dissolution in water are presented as three parallel reactions (Eqs. 10–12), and each reaction occurs in consecutive steps as

$$\mathrm{CaMg(CO_3)_2(s)} \rightarrow \mathrm{MgCO_3(s)} + \mathrm{Ca^{2+}} + \mathrm{CO_3^{2-}} \tag{10}$$

$$\mathrm{MgCO_3(s)} \rightarrow \mathrm{Mg^{2+}} + \mathrm{CO_3^{2-}} \tag{11}$$

Combine reaction (10) and reaction (11), then

$$\mathrm{CaMg(CO_3)_2(s)} \rightarrow \mathrm{Ca^{2+}} + \mathrm{Mg^{2+}} + 2\mathrm{CO_3^{2-}}$$

where the reaction (11) is a slow reaction, and also the reaction could occur as follows:

$$\mathrm{CaMg(CO_3)_2(s)} + \mathrm{Mg^{2+}} \rightarrow \mathrm{Ca^{2+}} + 2\mathrm{MgCO_3(s)} \tag{12}$$

And also, the following reaction occurs in the experimental system:

$$\mathrm{CO_3^{2-}} + \mathrm{H_2O} = \mathrm{HCO_3^-} + \mathrm{OH^-} \tag{13}$$

The following rate equation was used to describe overall rate of dolomite dissolution,

$$\text{Rate} = \Sigma r_{ij} = \Sigma k_{ij}(a_i)^n \tag{14}$$

where Σr_{ij} refers to one of each reaction among the above reactions; k_{ij} is the rate constant for ith species in the jth reaction, a_i stands for activity of ith aqueous species, n is the stoichiometric coefficience of ith species in the jth reaction, and define $n = n_{ij}$.

Berner and Morse (1974) presented an equation for calcite dissolution process as follows:

$$\text{Rate} = k_1 a_{\mathrm{H^+}} + k_2 a_{\mathrm{H_2CO_3}} + k_3 a_{\mathrm{H_2O}} + k_4 a_{\mathrm{Ca^{2+}}} a_{\mathrm{CO_3^{2-}}} \tag{15}$$

This rate equation could be applied to illustrate the release rate of $CaCO_3$ sites in dolomite dissolution processes. Through experiments we found dissolved Ca would inhibit dolomite dissolution over a wide temperature range from 25 to 250°C. In this study, authors do not change pH of the input solutions. Concerning the reaction (Eq. 10) to reaction (Eq. 11) that occurred in the system, HCO_3^- and CO_3^{2-} in reaction systems are dependent on the concentrations of dissolved Ca and Mg. Thus, we predict that overall dissolution rates will mainly related to activities of dissolved Ca and Mg (Dreybordt et al. 1996).

3.2 Incongruent Dissolution

The concentrations of Ca and Mg in the input solutions are zero, i.e., $C_0 = 0$. The concentrations (mol/l) of the dissolved Ca and Mg, C_i in the output aqueous solutions at each flow rate and at various temperatures were measured and $C_i - C_0 = C_i$. The molar concentration ratio between Ca and Mg in aqueous solutions, $(\mathrm{Ca/Mg})_{\mathrm{aq}}$ is different from its molar ratio in bulk solid $(\mathrm{Ca/Mg})_{\mathrm{solid}}$ which equal to 1.17 (Table 1).

Ca releases from solid and enters to solution often faster than Mg does as shown in Fig. 2. Dissolution of dolomite is incongruent in most cases, especially at temperatures above 100°C. Figure 2 shows that molar concentrations of dissolved Ca are covariant with Mg molar concentrations of the output solutions at temperatures below 150°C, which vary

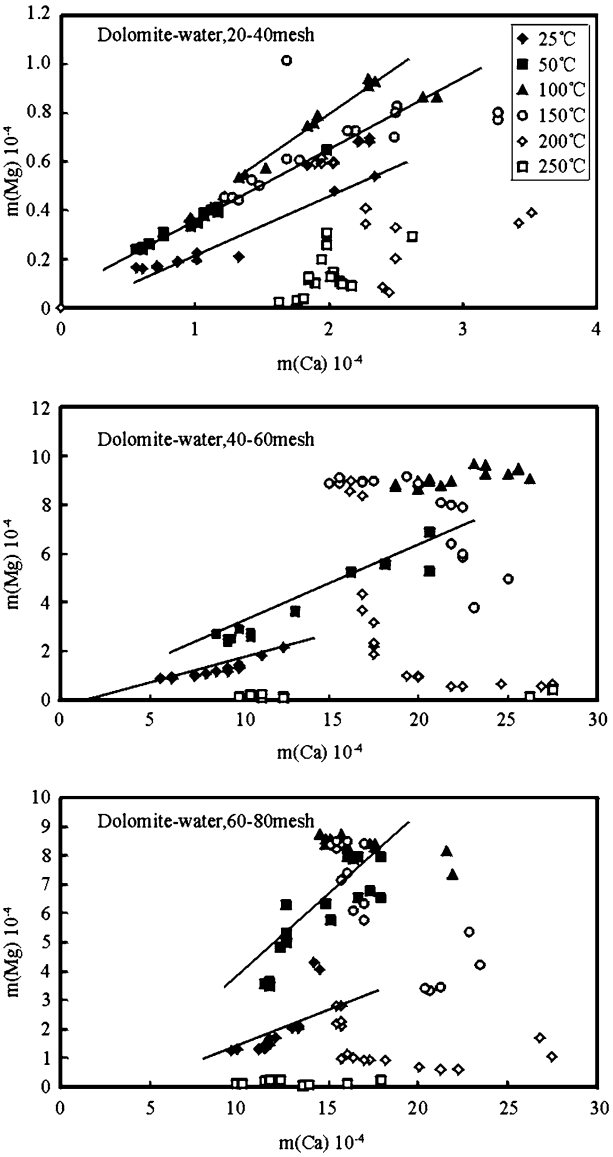

Fig. 2 The output solution Mg concentrations as a function of the corresponding output solution Ca concentrations. The symbols represent measured solution composition at 25, 50, 100, 150, 200, and 250°C. The linear relations show the concentration ratios of dissolved Ca/Mg in solutions at lower temperatures from 25 to 150°C for sample passed through 20–40 mesh. Linear relations show Ca/Mg release ratio at temperatures from 25 to 50°C for samples passed through 40–80 mesh

with mineral particle size. The correlation slopes in Fig. 2 show Ca/Mg molar concentration ratios in aqueous solutions, which generally level out to a constant value ranging from 2.5 to 5 at temperatures from 25 to 150°C for 20–40 mesh samples. For 40–60 mesh samples, Ca/Mg molar ratios in aqueous solutions vary from about 3–6 at temperatures from 25 to 50°C. For 60–80 mesh sample, Ca/Mg molar concentration ratios in aqueous

solutions varies from about 2.3–6 at temperatures from 25 to 50°C. At low temperatures (25–150°C for sample through 20–40 mesh), experiments show linear correlations between concentrations of Ca and concentrations of Mg in aqueous solutions, and concentrations of dissolved Mg are always lower than Ca, depicted in Fig. 2. At low temperatures (25–150°C), incongruent dissolution leads to non-stoichiometric surface leaching layer on dolomite.

Oppositely, at high temperatures ranging from 200 to 250°C for sample through 20–40 mesh, at temperatures from 100 to 250°C for 40–60 mesh and 60–80 mesh, the concentrations of dissolved Ca is not a linear correlation with Mg concentrations in output solutions. Dolomite dissolution varies with temperature, but at high temperatures Ca release to solution do not covary with release of Mg (Sect. 4.2). At these temperatures, incongruent dissolution is caused by a backward reaction, such as reaction (12), $MgCO_3$ precipitated on dolomite surface.

3.3 Rate Calculation

In the flow through experimental reactor the dissolution rate of the mineral (mol/min/m^2, or mol/s/m^2) leads to the following mass balance expression for the concentration of the ith solute in a reactor cell:

$$dC/dt = \text{Rate}\, v\,(A/V) - (C_i - C_0)/t \tag{16}$$

where v refers the stoichiometric coefficient of the ith solute in the mineral, A is the total reactive surface area of the mineral (m^2), t is the average residence time in pressure cell, V is the volume of the solution in the pressure vessel (ml). As $dC/dt = 0$, which means the steady state kinetic dissolution, then Rate is normalized with respect to stoichiometric coefficient and surface area/volume ratio, here $v = 1$,

$$\text{Rate} = \frac{C_i - C_0}{t(A/V)} \tag{17}$$

The calculation method of dissolution rate was reported before (Cama et al. 1999; Dove 1990; Hellmann 1995; Zhang et al. 1989).

3.4 The Release Rate Distributions Respect to Temperatures

3.4.1 Release Rate of Ca and Mg

Ca and Mg release rates in aqueous solutions were measured as functions of temperature in reaction systems, shown in Fig. 3. The maximum release rates of Ca and Mg of dolomite dissolution in the flowing hydrothermal systems under different flow velocities were always obtained at 200°C for 20–40 mesh sample. And the maximum release rates of Ca and Mg were found at 100–150°C for 40–60 mesh and for 60–80 mesh sample. The dissolution rates for 20–40 mesh dolomite increase with temperature rising from 25 to 200°C, but decrease with temperature increasing from 200 to 300°C (Fig. 3, Table 2). For 40–60 mesh and 60–80 mesh, dissolution rates increase with increasing temperatures until 100°C, then, they decrease with continued increasing temperatures from 100 to 250°C.

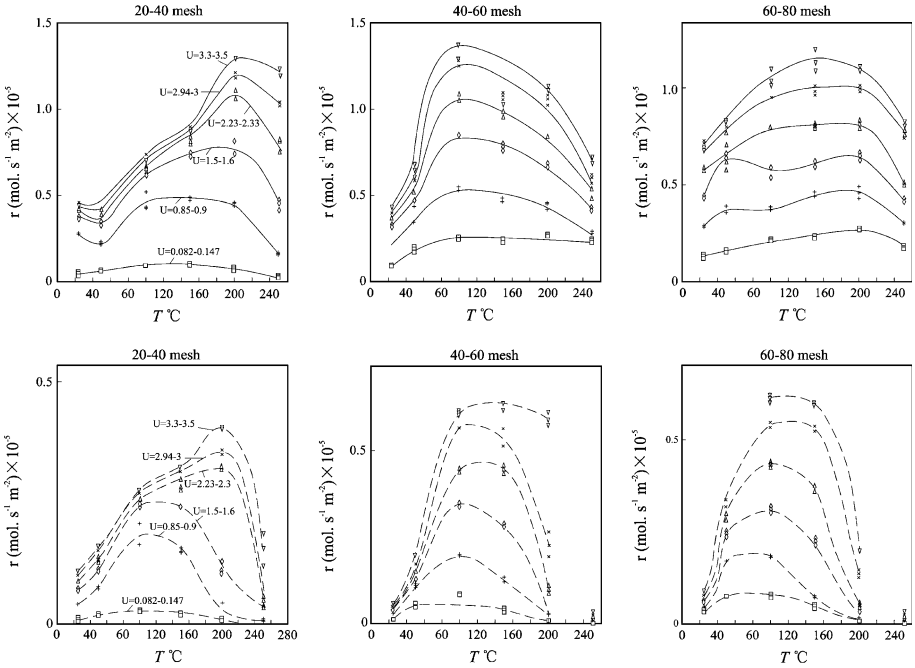

Fig. 3 The release rate of Ca and Mg as a function of temperature from 25 to 250°C. The release rates for Ca and Mg for three grain size samples varied in different flow velocities are depicted. The dashed lines are smoothed of the rate data

Dissolution product of fresh dolomite is often non-stoichiometric in most cases, and the molar concentration Ca/Mg ratio of dissolved species in the output solution was greater than Ca/Mg ratio in the bulk solid. The Ca/Mg ratio in solution increases with rising temperatures from 25 to 250°C. The release rates of Mg are usually lower than release rates of Ca at the same condition in most cases (Fig. 3). The release rate ratio R(Ca)/R(Mg) is also affected by temperature, shown in Fig. 4. Generally, R(Ca)/R(Mg) increase with increasing temperatures. Release rates of $MgCO_3$ sites in dolomite decrease with increasing temperature.

3.5 Effect of Dissolved Ca and Mg on the Dissolution Rates as a Strong Inhibitor

With increasing concentrations of dissolved Ca (or Mg) in the reaction solution, the dissolution rate of dolomite usually decreases from an initial value for a run progressively. As the concentration of Ca of the reaction solution reaches a high value, then the release rate of Ca becomes small in the temperature range of 25–250°C. For sample passed through 20–40 mesh, release rates of Ca and Mg also decrease with increasing concentration of dissolved Mg at low temperatures simultaneously. But at high temperatures from 200 to 250°C, the release rate of Ca and Mg increase with increasing the concentration of dissolved of Mg in some cases, shown in Fig. 5.

For 40–60 mesh and for 60–80 mesh samples, release rates of Ca or Mg decrease with increasing Ca concentrations over the temperature range from 25 to 250°C. In the

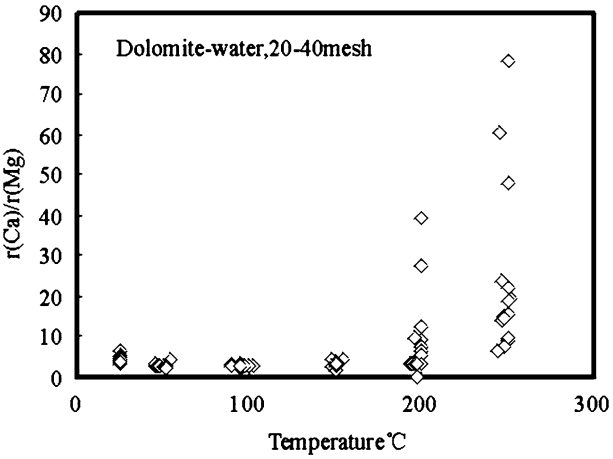

Fig. 4 The release rate ratio between Ca and Mg as a function of temperature

temperature range from 25 to 100°C, the release rates of Ca and Mg decreases with increasing concentration of dissolved Mg. But release rate of Ca and Mg increases with rising dissolved Mg in the outflow solution in some cases at 150 and 250°C.

The experiments prove that dissolved Ca is a strong inhibitor for dolomite dissolution (release of Ca) in most cases. But dissolved Mg is an inhibitor for dolomite dissolution at low temperatures. At high temperatures (200 to 250°C for sample through 20–40 mesh), dissolution rates of dolomite increase with increasing the concentration of dissolved Mg.

4 Discussion

4.1 Rate Equation

In order to interpret the role of dissolved Ca (Mg) as a strong inhibitor for dolomite dissolution, many investigators applied the saturation index values (sid) to illustrate what factor is controlling the dissolution rate of dolomite (Busenberg and White 1982, 1986; Herman and White 1985; Pokrovsky and Schott 2001) (Appendix 1).

As an empirical reaction rate expression obtained for calcite dissolution experiments (Holdren and Speyer 1985; Lasaga 1981, 1984; Morse 1983; Posey-Dowty et al. 1984; Sjöberg and Rickard 1983; Zhang et al. 1990a, b), its deviation from equilibrium can be expressed as

$$-r = \mathrm{d}C'/\mathrm{d}t = k\,Sa(C_s - C_i) \tag{18}$$

where Sa refers to surface area (unit with m^2/g); C_s is the saturation concentration of a dissolving species. C_i is the concentration of the species i, such as Ca. $(C_s - C_i)$ can be also expressed as the saturation index value as well as $(K_s - Q)$, i.e., the difference between the solubility product K_s, and the ion activity product Q (Morse 1983; Lasaga 1981) (Appendix 1).

The Eq. 18 can describe an elementary reaction, which is easy to illustrate the dissolution kinetics at how far from equilibrium state. The overall dissolution rate for dolomite is equal to the sum of the rates of each parallel elementary reaction, as previously reported (Busenberg and Plummer 1982; Chou et al. 1989).

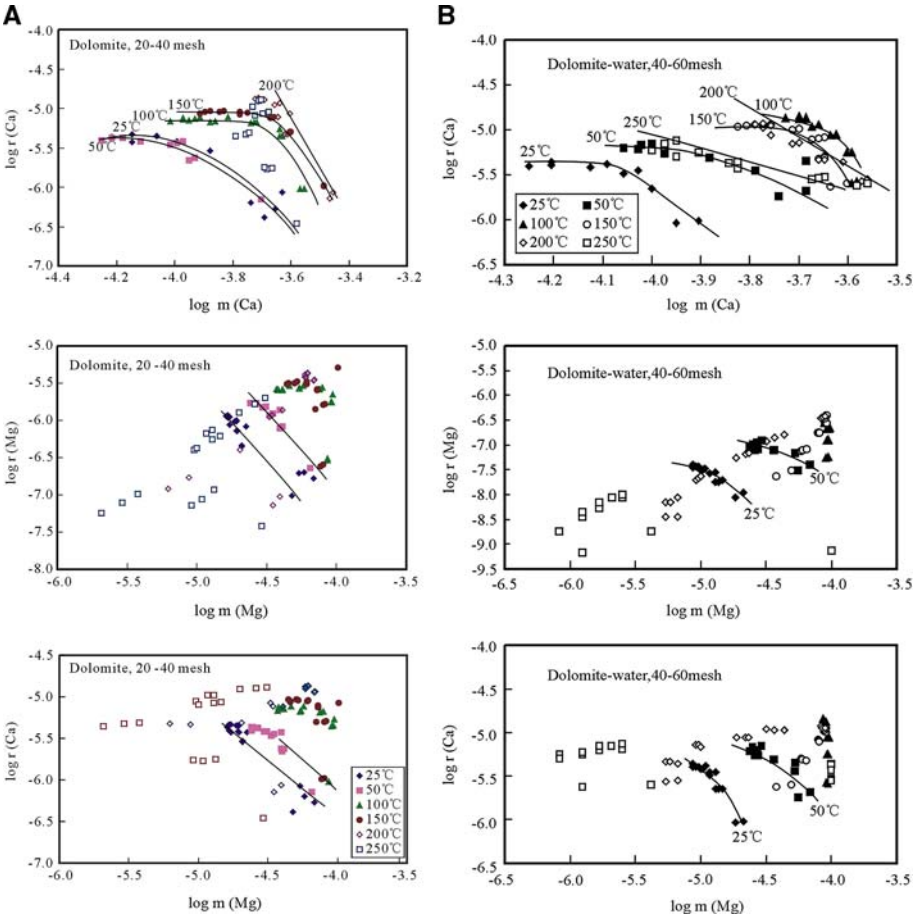

Fig. 5 Logarithms of dolomite dissolution rates (release rate of Ca and Mg) from 25 to 250°C depicted as a function of the logarithm of molality of dissolved Ca and Mg: (**A**) Dolomite particle passed through 20–40 mesh (a) log r(Ca) versuss log m(Ca), having trendlines of 25°C, 50°C, 100°C, 150°C, and 200°C; (b) log r (Mg) versus log m(Mg) having 25 and 50°C trendlines; (c) log r (Ca) versus log m(Mg) having 25 and 50°C trendlines. These trendlines show the correlations between logarithms of release rates of Ca (or Mg) and logarithms of molar concentrations of Ca (or Mg). (**B**) Dolomite particle passed through 40–60 mesh. See Table 3 for more detail about the correlation lines. There are also trendlines showing the correlations between logarithms of release rates of Ca (or Mg) and logarithms of molar concentrations of Ca (or Mg)

The chemical affinity of the overall hydrolysis reaction A can be also used to express the overall dissolution rate,

$$A = -RT\ln(Q/K_s) \tag{19}$$

and

$$\text{Rate} = r_+(1 - \exp(-A/\sigma RT)) \tag{20}$$

where r_+ is forward reaction rate. σ stands for Terkim's average stoichiometric number, which is equal to the ratio of the rate of activated or precursor complex destruction relative

Table 3 Rate law of the release rates of Ca and Mg, $-r_i = k(a_i)_i^n$ (calculation according to log $r_i = n_i \log(a_I) + \log k$)

	n (Ca)	Correl.	Log k (Ca)	n (Mg)	Correl.	Log k (Mg)
20–40 mesh						
25°C	−0.465	−0.83*	−6.05	−0.499	−0.9	−7.18
50°C	−0.646	−0.87	−6.88			
100°C				−0.473	−0.93	−5.31
150°C	−0.164	−0.81*	−5.20			
200°C	−0.182	−0.95	−4.36	0.43	0.84*	−2.33
250°C				0.498	0.81*	−2.33
40–60 mesh						
25°C	−0.42	−0.81*	−5.09	−0.55	−0.95	−7.16
50°C	−0.64	−0.84*	−5.8			
100°C	−0.18	−0.88	−3.43			
150°C				0.28	0.98	−1.72
200°C	−0.36	−0.98	−4.26	0.62	0.98	−0.28
250°C	−0.86	−0.96	−6.19	0.62	0.98	−0.77
60–80 mesh						
25°C	−0.19	−0.89	−3.81	−1.1	−0.91	−9.97
50°C						
100°C	−0.22	− 0.96	−3.76			
150°C	−0.26	−0.91	−3.88	0.33	0.92	−1.53
200°C	−0.41	−0.96	−4.53	0.44	0.85*	−1.34
250°C				0.45	0.82*	−0.83

Note: * means in some cases, the correlation coefficient between log r_{Ca} versus log $m_{Ca^{2+}}$ as well as the relation between log r_{Mg} versus log $m_{Mg^{2+}}$ is not very high that indicates the dissolution mechanism is more complex

to the overall dissolution rate. The chemical affinity can be also to express the reaction system and how far from the equilibrium.

At far from equilibrium conditions, $A \gg \sigma RT$, then Rate $= r_+$.

The forward reaction rate of a mineral dissolution is also assumed to be equal to product of the precursor complex (P^*) (Wieland et al. 1988; Stumm and Wieland 1990).

$$r_+ = k_+ P^* \tag{21}$$

Similarly, the overall reaction is equal to the sum of the rates of each parallel elementary reaction. Concerning to Eqs. 10–12, a general form of rate law can be expressed as

$$\text{Rate} = \Sigma k_{ij}(a_i)^n \tag{14a}$$

4.2 Dissolved Ca and Mg in Rate Equation at Far from Equilibrium

As mentioned above, rate equation of dolomite dissolution can be expressed as function of dissolved Ca and Mg.

$$-r_i = k_i(a_i)_i^n \tag{14b}$$

The rate equation could illustrate and interpret what factors affect *i*th reaction in dolomite dissolutions. The relation $\log r_i = n_i \log(a_i) + \log k$ can be used to find out whether a linear relationship exists between log r_i and log (a_i), which are depicted in Fig. 5. Linear regression methods may also be used to process data before calculating and obtaining the reaction rate constant k, and the order of reaction n (Table 3).

At 25°C for 20–40 mesh sample, the release rate of dissolved Ca, $-r(\mathrm{Ca}) = 10^{-6.05}(m_{\mathrm{Ca}^{2+}})^{-0.465}$; at 50°C for 20–40 mesh sample, $-r(\mathrm{Ca}) = 10^{-6.88}(m_{\mathrm{Ca}^{2+}})^{-0.646}$; at 150°C for 20–40 mesh sample, $-r(\mathrm{Ca}) = 10^{-5.2}(m_{\mathrm{Ca}^{2+}})^{-0.164}$; at 25°C for 40–60 mesh sample, $-r(\mathrm{Ca}) = 10^{-5}(m_{\mathrm{Ca}^{2+}})^{-0.42}$; at 50°C for 40–60 mesh sample, $-r(\mathrm{Ca}) = 10^{-5.8}(m_{\mathrm{Ca}^{2+}})^{-0.64}$; at 100°C for 40–60 mesh sample, $-r(\mathrm{Ca}) = 10^{-3.43}(m_{\mathrm{Ca}^{2+}})^{-0.18}$; at 25°C for 60–80 mesh sample, $-r(\mathrm{Ca}) = 10^{-3.81}(m_{\mathrm{Ca}^{2+}})^{-0.19}$; at 100°C for 60–80 mesh sample, $-r(\mathrm{Ca}) = 10^{-3.76}(m_{\mathrm{Ca}^{2+}})^{-0.26}$.

If Fig. 5 analyzed carefully, we find that the release rates of Ca remain a constant when the concentration of dissolved Ca, m_{Ca} increases until m_{Ca} reaches a value. For sample passed through 20–40 mesh, at $T = 25$ and $T = 50$ °C, if $\log m_{\mathrm{Ca}} \leq -4$, the release rate is not related to m_{Ca}, $-r = k_+$, which is typically at far from equilibrium. When log $m(\mathrm{Ca}) > -4$, release rate decreases with continued increasing m_{Ca}, $-r = k_+ (m_{\mathrm{Ca}})^n$. Similarly release rates are not related to m_{Ca}, release rate $= k_+$ when $\log m_{\mathrm{Ca}} \leq -3.72$ at $T = 100$°C, and $\log m_{\mathrm{Ca}} \leq -3.65$ at $T = 150$°C. At $T = 200$°C, release rate $= k_+ (m_{\mathrm{Ca}})^n$. Release rates of Ca (or Mg) decrease with increasing m_{Mg} at $T = 25$ and 50°C.

For samples passed through 40–80 mesh, we also find that release rates of Ca remain a constant when the concentration of dissolved Ca, $m_{\mathrm{Ca}^{2+}}$ increases until m_{Ca} reaches a special value, then release rate decreases with continued increasing concentrations of Ca at $T = 25$°C, 50°C, 100°C, and 150°C, and release rates decrease with increasing $m_{\mathrm{Ca}^{2+}}$ at $T = 200$°C and 250°C, shown in Fig. 5B.

Figure 2 provides evidence that at low temperatures of 25–150°C for low surface area sample (passed through 20–40 mesh) and at temperatures of 25–50°C for 40–60 and 60–80 mesh samples, the molar concentration ratios between dissolved Ca and Mg in output solutions are almost constant at each temperature, then the release rate of Mg can be figured out from the rate law of release of Ca. That means release rate ratio of Ca/Mg is constant at each temperature from 25 to 150°C. And also, Table 3 indicates that the release rate law for Ca (or Mg) is different among the three grain size samples.

Although incongruent dissolution of dolomite occurs in the temperature range from 25 to 150°C for low surface area sample (and 25–50°C for sample passed through 40–80 mesh), the non-stoichiometric surface layer happens to dolomite surface and it is a stable, Mg rich leaching layer at each temperature. At low temperatures (25–150°C), incongruent dissolution leads to non-stoichiometric surface layer on dolomite. Oppositely, at high temperatures (200–250°C for sample passed through 20–40 mesh), incongruent dissolution would cause developing secondary phase-$MgCO_3$ on dolomite surface, as expressed in the reaction (12).

4.3 Mg Adsorption

At temperatures $\geq$200°C for 20–40 mesh, at temperatures $\geq$150°C for 40–60 mesh and for 60–80 mesh, an increase of the concentration of dissolved Mg favors increasing release of Ca and Mg. As mentioned before, the covariance of R(Ca) with (Mg) behave in a more complex form at high temperatures (Fig. 5). Assumed the following reaction occurred in dolomite dissolution system,

$$CaCO_3\,(\text{in dolomite}) + Mg^{2+} = Ca^{2+} + MgCO_3\,(\text{in dolomite}) \quad (12)$$

It is reasonable to consider that the above reaction is the step controlling dissolution of dolomite at high temperatures, and that a cation Mg^{2+} adsorption process will be involved in the dolomite dissolution.

Quantifying a model to describe incongruent dissolution rates of dolomite in water becomes more difficult when the Mg ions are adsorbed on mineral surface, which affected $CaCO_3$ dissolution, involved in the rate-limiting step. Some scientists have presented a model for mineral dissolution in electrolyte solutions that a cation adsorption favors to increase dissolution rates of minerals (Rimstidt and Dove 1986; Dove and Crerar 1990; Icenhower and Dove 2000).

However, if the release rates of $CaCO_3$ in dolomite were related to the concentration of magnesium ions in solution, then a Langmuir model for equilibrium adsorption can be used to describe the dissolution rate law of dolomite. This method has been applied before (Rimstidt and Dove 1986; Blum and Lasaga 1988, 1991; Dove and Crerar 1990). This model gives the relation between the reactivity of the adsorbate and the amount adsorbed where each exposed C–O group represents one adsorption site and all sites are assumed to have equal energy. This assumption is probably valid for dolomite since sites located at edges and defects probably have higher reactivities. But their contribution does not control the overall rate constant (Blum and Lasaga 1988, 1991). The reaction rate is directly proportional to the number of sites and the frequency at which the cation adsorbs onto the sites and increases the accessibility of water molecules, as follows

$$r = k_{ad}\theta_i \quad (22)$$

where r = reaction rate for the adsorption mode (mol m^{-2} s^{-1}); k_{ad} = rate constant for the adsorption mode (mol m^{-2} s^{-1}); θ_i = fraction of occupied sites. Using magnesium ion as an example, the Langmuir isotherm describes θ_i and is given by

$$\theta_i = (K_{Mg^{2+}} m_{Mg^{2+}})/(1 + K_{Mg^{2+}} m_{Mg^{2+}}) \quad (23)$$

where $m_{Mg^{2+}}$ = concentration of magnesium ion (molal); $K_{Mg^{2+}}$ = equilibrium adsorption coefficient ($molal^{-1}$). Thus, the equation describing a process limited by a reaction at the surface is given by

$$-r = k_{ad}\,((K_{Mg^{2+}} m_{Mg^{2+}})/(1 + K_{Mg^{2+}} m_{Mg^{2+}})) \quad (24)$$

$$\frac{1}{r} = \left[\left(\frac{1}{k_{ad}}\right)\left(\frac{1}{k_{Mg^{2+}}}\right)\right]\frac{1}{m_{Mg^{2+}}} + \frac{1}{k_{ad}} \quad (25)$$

which can be transformed into a linear form and allows the values of the constants, k_{ad} and K_{Mg} to be extracted from the slope and intercept of a weighed least squares fit to the experimental data. Table 4 gives these Langmuir constants (of magnesium adsorption) for the dissolution of dolomite over the temperature range 25–250°C in water. Figure 6 depicted the linear relations between $1/r$ and $1/m_{Mg}$ in the case of dolomite dissolution in the temperature range 200–250°C.

So far, the release rates of $CaCO_3$ in dolomite in degassed and de-ionized water have been considered to relate to the concentrations of dissolved Ca (or activity product, $a_{CO_3^{2-}} a_{Ca^{2+}}$ and to adsorption of magnesium ions, separately, but these effects can be combined to give a general rate equation. First, the response of the dissolution rate constant to the addition of Mg, follows the form

Table 4 k_{Mg} and K_D of dolomite dissolution at high temperature

Sample (mesh)	Temperature (°C)	Rate constant for the adsorption mode k_{Mg} (mol m^{-2} s^{-1}) × 10^4	Equilibrium adsorption coefficient K_D ($molal^{-1}$)	Correlation coefficience
20–40	200	6.75 (5.3–9.7)	0.015 (0.01–0.0175)	0.928
	250	20.55 (14–28)	0.014 (0.01–0.019)	0.956
40–60	150	−0.065 (−0.60 to 0.72)	−0.076 (−0.06 to 0.075)	0.978
	200	8.18 (6–9)	0.14 (0.09–0.19)	0.964
	250	195.55 (173–219)	0.085 (0.08–0.09)	0.869
60–80	150	0.24 (0.1–0.67)	0.32 (0.2–1.4)	0.9436
	200	4.88 (2–5.6)	0.24 (0.1–0.5)	0.931
	250	−62.44 (−28 to 95)	0.02 (0.01–0.03)	0.829

$$k_{total} = \left(k_+ + k_{ad}\frac{K_{me^+}m_{me^+}}{1 + K_{me^+}m_{me^+}}\right) \tag{26}$$

where k_{total} = net rate constant for dissolution in pure water (mol m^{-2} s^{-1}). m_{me^+} refers to molal concentration of magnesium ion. K_{me^+} is the same as $K_{Mg^{2+}}$. This rate equation is suitable to dolomite dissolutions at high temperatures from 200 to 250°C for 20–40 mesh, and at temperatures from 150 to 250°C for 40–80 mesh sample.

Concerning reactions from (10) to (12), the overall dissolution rate of dolomite can be described as follows:

$$\text{Rate} = k_{10} + k_{11} + k_{12}\,a_{Mg^{2+}} \tag{14c}$$

The k_{10} refers to surface hydration of $CaCO_3$ sites in dolomite, k_{11} stands for surface hydration of $MgCO_3$ sites in dolomite, and $k_{12}\,a_{Mg^{2+}}$ approximately accounts for reaction corresponded to Mg^{2+} adsorption on dolomite surface.

We predict that release rates of Ca of overall dissolution involve k_{10} and $k_{12}\,a_{Mg^{2+}}$. And k_{10} is related to dissolved Ca $m_{Ca^{2+}}$ and $k_{12}\,a_{Mg^{2+}}$ is related to dissolved Mg, then, release rates at high temperatures.

$$-r = k(m_{Ca^{2+}})^n + k_{ad}(K_{Mg^{2+}}m_{Mg^{2+}})/(1 + K_{Mg^{2+}}m_{Mg^{2+}}) \tag{27}$$

But, at low temperatures and low dissolved Ca, release rates of Ca, $-r = k_{10} = k_+$, as mentioned in Sect. 4.2.

Therefore, Mg ion absorption on dolomite surface affects the overall rates of dolomite dissolution particularly at high temperatures. A surface complex involving Mg could occur on surface, as reported by Pokrovsky and Schott (2001).

According to the Tables 3 and 4, we can obtain the $k(m_{Ca})$, k_{ad} and K_{Mg}, and then describe the dissolution rate law of dolomite in water in the temperature range from 150°C to 250°C. For example, in the case of 200°C for 40–60 mesh sample, the release rate of Ca can be described as:

$$-r(\text{mol}\,m^{-2}s^{-1}) = 0.55 \times 10^{-4}(m_{Ca^{2+}})^{-0.36} + 0.135 \times 10^{-4}(m_{Mg^{2+}})/(1 + 0.14\,m_{Mg^{2+}}) \tag{28}$$

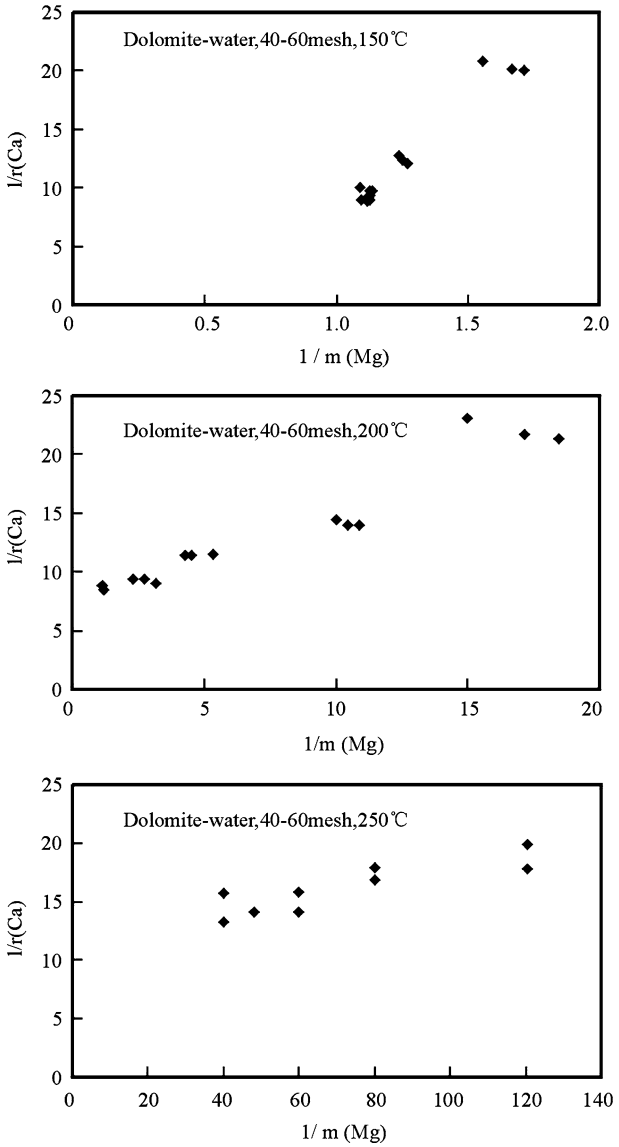

Fig. 6 Plot of $1/r$ as a function of $1/m_{Mg}$ for 20–40 mesh sample in the temperatures 150°C, 200°C and 250°C

4.4 Temperature Effects on Dissolution

Arrhenius-type plot is constructed to take into account the dependence of initial rate constant on temperature. Figure 7 shows the Arrhenius type plot for $d(\ln k)/d(1/T)$ of three kinds of dolomite samples, which is constructed using the dependence of release rate constants of Ca (or Mg) on temperature for three kinds of samples.

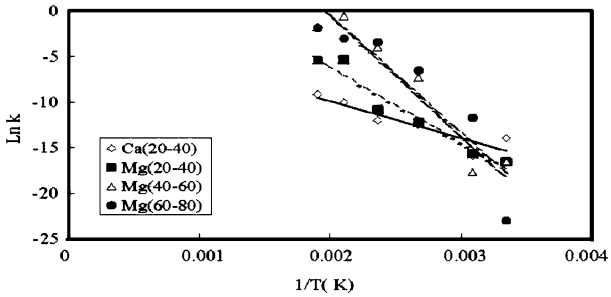

Fig. 7 Arrhenius plots of ln Rate versus $1/T$ (°K) for dolomite in the temperature range from 25 to 250°C. Rate refer to the release rates of Ca (20–40 mesh), release rates of Mg (20–40 mesh), release rates of Mg (40–60 mesh) and release rates of Mg (60–80 mesh)

And the activation energy (*Ea*) of the overall reaction, is given by

$$\mathrm{d}(\ln k)/\mathrm{d}(1/T) = -(Ea/R) \tag{29}$$

where R refers to gas constant (8.314 J mol^{-1} K^{-1}). For samples passed through 20–40, 40–60 and 60–80 mesh in the temperature range from 25 to 250°C, the overall *Ea* for release rates of Ca and Mg are similar to values published by Herman and White (1985) and Busenberg and Plummer (1982) (Table 5).

Table 5 Activation energies calculated from release rate constant for Ca and Mg of dolomite dissolution in the temperature range from 25 to 250°C

Sample	Rate	*Ea* (kJ mol^{-1})
*Herman and White*1985		
	Spining rate (rpm)	0, 15, 25°C
Bellfonte	900	34
Bellfonte	225	32
Bellfonte	28	32
Single crystal	225	27
Busenberg and White 1982[a]		
		25, 50, 100°C
Sedimentary	k_1	30.5
	k_2	29.3
	k_3	39.7–54.8
Hydrothermal	k_1	51.9–89.3
	k_2	51.0–77.6
	k_3	67.8–139
This study[b]		
Sample size		25–250°C
20–40 mesh	k of Ca release rate	33.197
20–40 mesh	k of Mg release rate	69.045
40–60 mesh	k of Mg release rate	104.67
60–80 mesh	k of Mg release rate	108.24

Note: [a] Busenberg and White (1982) described k_1, k_2, k_3

[b] For 40–60 mesh and for 60–80 mesh samples, the release rate of Ca seems to not have good correlation to the Ca concentration

Table 5 shows that the activation energies are different among three particle size experiments. The experimental results demonstrate that the theoretical model predicted by Buhmann and Dreybrodt (1985a, b) is correct, that the dissolution rates depend critically on the ratio of the volume V of the solution and the surface area of the reacting mineral, V/A, in the reaction system. Therefore, dolomite dissolution rates vary with respect to particle size.

5 Application: Diagenesis of Dolomite in Water

Experimental results bring new light on dolomite behavior in aquatic systems, especially in epithermal system. As reported before, the inhibiting effect of Ca on dolomite dissolution could be used to explain the high stability of dolomite in many sedimentary environments (Pokrovsky and Schott 2001). The conversion of dolomite into calcite under the influence of Ca-rich solutions is very sluggish. This study indicates that this conversion at high temperatures is almost impossible.

This study suggests two important results, the release rate ratio of R(Ca)/R(Mg) increases with temperature and Mg adsorption rate increases with temperature. And also, dissolution rates of dolomite decrease with rising temperature at temperature above 200°C for coarse grain sample (passed through 20–40 mesh), and they decrease with increasing temperature at temperature above 150°C for fine grain sample (passed through 40–80 mesh). These facts demonstrate dolomitization occurs often at high temperatures, better above 200°C. Experiments indicate that release rate of Ca (or Mg) for coarse grain dolomite (20–40 mesh) is usually lower than that for fine grain dolomite (40–80 mesh). Also, the R(Ca)/R(Mg) is different among the different grain sizes. It can illustrate those facts the epithermal and low grade metamorphism that always cause the rock re-crystallization, which accompanies dolomitization.

6 Conclusion

The dissolution kinetics of dolomite is quantified across the temperature range of 25–250°C by using a flow through reactor of open system. This study provides various dissolution rate data employed at a wide variety of experimental temperatures, as well as different particle size samples, which passed through 20–40 mesh, 40–60 mesh, and 60–80 mesh. The experimental data show that the dissolution rates of dolomite vary with respect to particle size and temperatures.

Our experimental results indicate that the dissolution of dolomite is strong incongruent in water in the temperature range from 25 to 250°C. The molar concentration ratio of Ca/Mg in output solutions varied from 2 to 6 in the temperature range from 25 to 150°C and the ratio is constant at each temperature. The molar concentration ratios of Ca/Mg in solutions are larger than the molar ratio Ca/Mg in solid, 1.17. At low temperatures of 25– 150°C for low surface area sample (20–40 mesh sample) and at 25–100°C for samples passed through 40–60 and 60–80 mesh, concentrations of dissolved Ca in output aqueous solution are proportional to Mg concentrations. Non-stoichiometric dissolution products are derived from non-stoichiometric leaching surface on dolomite at low temperatures of 25–150°C. At high temperatures, dissolved Ca does not covary with dissolved Mg. Release of $MgCO_3$ sites in dolomite is the slow reaction step. And also, reaction (12) seems to be important.

The release rates of Ca and Mg increase with increasing temperatures from 25 to 200°C for sample passed through 20–40 mesh, decrease with increasing temperature from 200 to

250°C. The maximum release rate of Ca (or Mg) is at 200°C. As to samples passed through 40–60 mesh and 60–80 mesh, the maximum release rate of Ca (or Mg) is at 100°C and 150°C. The ratio of the release rate of Ca over the release rate of Mg, R(Ca)/R(Mg) increases with increasing temperatures.

The dissolved Ca was found to inhibit dolomite dissolution in neutral water. The release rate of Ca, r_{Ca} (or r_{Mg}) decreases with increasing the concentration of dissolved Ca. The release rates decrease with increasing dissolved Mg at temperatures below 150°C. Experiments prove the logarithm of release rate of Ca covary with logarithm of molar concentration of Ca in most conditions. But log r_{Mg} covary with log m_{Mg} at low temperatures. For the multi-step reactions of dolomite dissolution, the rate law of release rates of Ca and Mg, Rate $= \Sigma k_{ij}(a_i)^n$ has been used to illustrate the dolomite dissolution behavior.

We found release rates of Ca of dolomite dissolutions increase with the increasing concentration of dissolved Mg at high temperatures above 150°C, and the adsorption reaction of Mg on the surface is the step to rate controlling. At high temperatures, non-stoichiometry of dissolved Ca and Mg in solutions is due to the dissolution of the original dolomite coupled to the precipitation of the secondary phase ($MgCO_3$).

The following rate equation is suitable to describe dolomite dissolutions at high temperatures from 200 to 250°C for sample passed through 20–40 mesh, and at temperatures from 150 to 250°C for sample passed through 40–80 mesh:

$$-r = k(m_{Ca^{2+}})^n + k_{ad}(K_{Mg^{2+}} m_{Mg^{2+}})/(1 + K_{Mg^{2+}} m_{Mg^{2+}}). \quad (27)$$

For example, at 200°C for mineral sample passed through 40–60 mesh, dissolution rate law for the release rate of Ca can be described as

$$-r(\text{mol m}^{-2}\,\text{s}^{-1}) = 0.55 \times 10^{-4}(m_{Ca^{2+}})^{-0.36} + 0.135 \times 10^{-4}\,(m_{Mg^{2+}})/(1 + 0.14\, m_{Mg^{2+}}). \quad (28)$$

The data reported herein for low temperature 25–100°C are in good agreement with previously published dolomite dissolution rates in water over the temperature range of 25–100°C (Herman and White 1985; Busenberg and Plummer 1982; Pokrovsky and Schott 2001).

Acknowledgments We would like to thank the Ministry of Science and Technology and the Ministry of Land and Resources for supporting our project. This study was supported by 2001AA612020-3, 2003AA612020-3; 2001DEA30041, 2002DEA30084, 2003DEA2C021; 2001DEA20023B; 20010302; and NSFC:40043011; 20373064 and DY105-0301.

Appendix 1: Saturation Index

The dolomite saturation index was defined as

$$\text{sid} = 1/2 \log (\text{Activity product of output aqueous species of Ca, Mg, } CO_3)/K_s \quad (A1)$$

where K_s, the thermodynamic solubility product of dolomite was also calculated by using Shvarov software HCh (Shvarov 1989).

Concerning the bulk concentration of the solution in which calcite dissolves, the difference between the solubility product K_s, and the ion activity product Q i.e.,

$$a_{CO_3^{2-}} a_{Ca^{2+}}$$

The ($K_s - Q$) could be also described for the distance of the system from equilibrium as well as saturation index (Morse 1983; Lasaga 1981; Sjöberg and Rickard 1983).

In general, to determine the correct rate law to use, experiments would be carried out at far from equilibrium. Thus, for calcite dissolution processes, the simplified form of the rate law can be described as

$$-r = k(T)Sa(a_{Ca^{2+}}a_{CO_3^{2-}} - K_S)^n \quad \text{(A2)}$$

References

Berner RA, Morse JM (1974) Dissolution kinetics of calcium carbonate in sea water IV. Theory of calcite dissolution. Am J Sci 274:108–134

Blum A, Lasaga AC (1988) Role of surface speciation in the low-temperature dissolution of minerals. Nature 331:431–433

Blum AE, Lasaga AC (1991) The role of surface speciation in the dissolution of albite. Geochim Cosmochim Acta 55:2193–2201

Buhmann D, Dreybrodt W (1985a) The kinetics of calcite dissolution and precipitation in geologically relevant situations of karst areas. 1. Open system. Chem Geol 48:189–211

Buhmann D, Dreybrodt W (1985b) The kinetics of calcite dissolution and precipitation in geologically relevant situations of karst areas. 2. Closed system. Chem Geol 53:109–124

Busenberg GE, Plummer LN (1982) The kinetics of dissolution of dolomite in CO_2-H_2O systems at 1.5 to 65°C and 0 to I atm PCO_2. Amer J Sci 282:45–78

Busenberg E, Plummer LN (1986) Comparative study of the dissolution and crystal growth kinetics of calcite and aragonite. In: Munpto FA (ed) Studies in diagenesis. USGS Bull 1578, pp 139–168

Cama J, Aypra C, Lasaga AC (1999) The deviation from equilibrium effect on dissolution rate and on apparent variations in activation energy. Geochim Cosmochim Acta 61:2481–2486

Casey WH (1987) Heterogeneous kinetics and diffusion boundary layer: the example of reaction in a fraction. J Geophys Res B92:8007–8014

Chou L, Garrels RM, Wollast R (1989) Comparative study of the kinetics and mechanisms of dissolution of carbonate minerals. Chem Geol 78:269–282

Dove PM, Crerar DA (1990) Kinetics of quartz dissolution in electrolyte solutions using a hydrothermal mixed flow reactor. Geochim Cosmochim Acta 54:955–969

Dreybrodt W, Lauckner J, Liu Z, Svensson U, Buhmann D (1996) The kinetics of the reaction $H_2O + CO_2 = H^+ + HCO_3^-$ as one of the rate limiting steps for the dissolution of calcite in the system H_2O-CO_2-$CaCO_3$. Geochim Cosmochim Acta 60(18):3375–3381

Hellmann R (1995) The albite-water system. Part II. The time-evolution of the stoichiometry of dissolution as a function of pH at 100, 200, and 300°C. Geochim Cosmochim Acta 59:1669–1697

Hellmann R, Crerar DA, Zhang R (1989) Albite feldspar hydrolysis to 300°C. Solid State Ionics 32/33: 314–329

Herman JS, White WB (1985) Dissolution kinetics of dolomite: effects of lithology and fluid velocity. Geochim Cosmochim Acta 49:2017–2026

Holdren GR, Speyer PM (1985) Reaction rate-surface area relationship during the early stages of weathering: l. Initial observations. Geochim Cosmochim Acta 49:675–681

Icenhower JP, Dove MP (2000) The dissolution kinetics of amorphous silica into sodium chloride solutions: effects of temperature and ionic strength. Geochim Cosmochim Acta 64(24):4193–4203

Lasaga AC (1981) Rate laws of chemical reactions, and transition state theory. In: Lasaga AC, Kirkpatrick (eds) Kinetics of geochemical processes. Rev Mineral Geochem 8, pp 1–68 and 135–169

Lasaga AC (1984) Chemical kinetics of water-rock interactions. J Geophys Res 89:4009–4025

Lund K, Fogler HS, McCune CC (1973) Acidization-I. The dissolution of dolomite in hydrochloric acid. Chem Eng Sci 28:691–700

Mogollon JL, Ganor J, Soler JM, Lasaga AC (1996) Column experiments and the complex dissolution rate law of gibbsite. Amer J Sci 296:729–765

Mogollon JL, Perez-Dial A, Monaco SL (2000) The effects of ion identify and ionic strength on the dissolution rate of a gibbsitic bauxite. Geochim Cosmochim Acta 64(5):781–795

Morphy MJ, Oelkers E, Lichtner P (1989) Surface reaction versus diffusion control of mineral dissolution and growth in geochemical processes. Chem Geol 78:357–380

Morse JW (1983) The kinetics of calcium carbonate dissolution and precipitation. In: Reeder RJ (ed) Reviews in mineralogy, vol 11. Mineralogical Society of America, Washington, DC

Plummer LN, Wigley TML, Parkhurst DT (1978) The kinetics of calcite dissolution in CO_2-water systems at 5°C to 60°C and 0.0 to 1.0 atm CO_2. Am J Sci 278:179–216

Pokrovsky O, Schott J (2001) Kinetics and mechanism of dolomite dissolution in neutral to alkailine solutions revisited. Am J Sci 301:597–628

Pokrovsky O, Schott J, Thomas F (1999) Processes at the magnesium bearing carbonate/solution interface. I. A surface speciation model of magnesite. Geochim Cosmochim Acta 63:863–880

Posey-Dowty J, Borcsik M, Crerar, Zhang R (1984) The dissolution kinetics of calcite from 25 to 300°C in aqueous solution. G.S.A., Annual meeting, Abstracts

Rimstidt JD, Dove P (1986) Mineral/solution reaction rates in a mixed flow reactor: wollastonite hydrolysis. Geochim Cosmochim Acta 50:2509–2516

Shvarov Yu W (1989) A numerical criterion for existence of the equilibrium state in an open chemical system. Sci Geol Bull 42(4):365–369, Strasbourg

Sjöberg EL, Rickard D (1983) Mixed kinetic control of calcite dissolution rate. Am J Sci 238(8):815–830

Sjöberg EL, Rickard D (1984) Calcite dissolution kinetics: surface speciation and the origin of the variable pH dependence. Chem Geol 42:119–136

Stumm W, Wieland E (1990) Dissolution of oxide and silicate minerals: rate depend on surface speciation. In: Stumm W (ed) Aquatic chemical kinetics. Wiley-Interscience, New York, pp 367–400

Weissbart EJ, Rimstidt JD (2000) Wollastonite: incongruent dissolution and leached layer formation. Geochim Cosmochim Acta 64(23):4007–4016

Wieland E, Werhli B, Stumm W (1988) The coordination chemistry of weathering. III. A potential generalization on dissolution rates of minerals. Geochim Cosmochim Acta 52:1969–1981

Wollast R (1990) Rate and mechanism of dissolution of carbonates in the system $CaCO_3$–$MgCO_3$. In: Stumm W (ed) Aquatic chemical kinetics. Wiley-Interscience, New York, pp 431–445

Zhang R, Hu S (1996) Dissolution reaction kinetics of fluorite in flow systems and its surface chemistry. Sci China D 39(6):561–575

Zhang R, Hu S, Posey-Dowty J, Hellmann R, Borcsik M, Crerar D (1989) Kinetic study of mineral-water reactions in hydrothermal flow systems at elevated temperatures and pressures. Sci China B 11:1212–1222 (English abstract)

Zhang R, Posey-Dowty J, Hellmann R, Borcsik M, Crerar D, Hu S (1990a) Kinetics of mineral-water reactions in hydrothermal flow systems at elevated temperatures and pressures. Sci China B 33(9):1136–1152 (English edition)

Zhang R, Posey-Dowty J, Hellmann R, Borcsik M, Crerar D, Hu S (1990b) Kinetics of mineral-water reactions in hydrothermal flow systems at elevated temperatures and pressures. Science China B 33(9):1136–1152 (English edition)

Zhang R, Hu S et al (1992) Book: chemical kinetics of minerals in hydrothermal systems and mass transfer. Science Published House, Beijing (Chinese with a detail abstract in English)

Zhang R, Hu S, Posey-Dowty J, Crerar D, Borcsik M (1993) Chemical kinetics of mineral dissolutions and mass transfer, Selected paper from international scientific and technological projects (1986–1990), International Exchange on Earth Sciences (XlV), Ed. by Division of foreign affairs, Chinese Academy of Geological Sciences, Geological Publishing House, Beijing, English abstract

Zhang R, Hu S, Tong J, Jiang L (1998) Mineral-fluid reaction kinetics in open systems. Science Publishing House, Beijing (detail English abstract)

Zhang R, Hu S et al (2000) Kinetics of hydrothermal reactions of minerals in near-critical and supercritical water. Acta Geol Sin 74:400–405

Zhang R, Hu S, Su Y (2002) Hydrothermal alteration zoning and kinetic process of mineral-water interactions. Acta Geol Sin 76:351–366